

Roles of DSCAM in axonal decussation and fasciculation of chick spinal interneurons

OKSANA COHEN¹, LILACH VALD¹, MASAHITO YAMAGATA², JOSHUA R. SANES² and AVIHU KLAR^{*1}

¹Dept. of Medical Neurobiology, IMRIC, Hebrew University-Hadassah Medical School, Jerusalem, Israel and

²Center for Brain Science, Harvard University, Cambridge, Massachusetts, USA

ABSTRACT The ventral midline of the embryonic neural tube, the floor plate, has a profound role in guiding axons during embryonic development. Floor plate-derived guidance cues attract or repel axons, depending on the neuronal subtype and developmental stage. Netrin-1 and its receptor, Deleted in Colon Carcinoma (DCC), are the key constituents of commissural axons guidance cues toward the floor plate. Recent studies have implicated Down Syndrome Cell Adhesion Molecule (Dscam) as an additional Netrin-1 receptor. In this study, we examined the role of Dscam in guiding defined spinal dorsal interneuron populations. *In vivo* knockdown and ectopic expression of Dscam were performed in the dorsal dl1, dl2 and dl3 interneurons of chick embryos, by separately increasing or decreasing Dscam expression in each of these three specific interneuronal populations. Neuron-specific gain and loss of function of Dscam had no effect on the axonal trajectories of dl1-3 neurons. The commissural neurons, dl1c and dl2, crossed the midline, and the ipsilaterally projecting neurons, dl1i and dl3, projected ipsilaterally. However, the fasciculation of dl1 axons was diminished when Dscam expression was attenuated. Dscam is not required for either attraction to or repulsion from the floor plate. In contrast, Dscam is required for the fasciculation of axons, probably via homophilic interaction.

KEY WORDS: *spinal cord, axon guidance, floor plate, DSCAM, fasciculation*

Introduction

In bilaterally symmetric vertebrates, the floor plate at the ventral midline plays a crucial role in directing axon growth during the formation of neuronal circuits within the central nervous system. Floor plate cells provide a variety of guidance cues for growing axons, that elicit divergent effects depending on the neuronal cell type or its developmental stage (Dickson and Zou, 2010, Evans and Bashaw, 2010). Biochemical, *in vitro* and genetic evidence has demonstrated that the floor plate protein, Netrin-1, and its axonal receptor, Fra/DCC, are a key ligand-receptor pair that guides axons toward the floor plate (Dickson and Zou, 2010; Evans and Bashaw, 2010; Kennedy *et al.*, 1994; Serafini *et al.*, 1996; Serafini *et al.*, 1994). In vertebrates, Shh and VEGF, which are expressed in the floor plate, and their axonal receptors, Boc, Ptc and Flk1, are additional attractive cues that synergize with netrin-1 in directing commissural growth cones toward the floor plate (Charron *et al.*, 2003, Okada *et al.*, 2006, Ruiz de Almodovar *et al.*, 2011).

The incomplete failure of commissural midline crossing in DCC mutant mice suggests that other receptors may convey the Netrin-1 signal (Fazeli *et al.*, 1997). Several biochemical and genetic results implicated the Down Syndrome Cell Adhesion Molecule (Dscam) as a receptor for Netrin-1 that participates in regulation of midline crossing: 1) Netrin-1 binds to Dscam and DCC at similar affinities (Andrews *et al.*, 2008, Liu *et al.*, 2009, Ly *et al.*, 2008). 2) Knockdown of Dscam by siRNA in mouse and chick embryonic neural tubes causes a substantial reduction in the number of commissural axons that cross the midline (Liu *et al.*, 2009, Ly *et al.*, 2008). 3) In an *in vitro* turning assay using rat neural tube explants, blocking either DCC or Dscam activity does not alter the turning of commissural axons within the neuroepithelium toward an exogenous Netrin-1 source, whereas blockade of both receptors prevents turning (Ly *et al.*, 2008). 4) In a similar assay using chick neural tube explants,

Abbreviations used in this paper: DCC, deleted in colon carcinoma; Dscam, Down Syndrome cell adhesion molecule.

*Address correspondence to: Avihu Klar, Dept. of Medical Neurobiology, IMRIC, Hebrew University-Hadassah Medical School, POB 12272, Jerusalem, Israel 91120, USA. Tel: 972-2-675-7133. Fax: 972-2-675-7451. E-mail: avihu@cc.huji.ac.il - web: <https://medicine.ekmd.huji.ac.il/En/Publications/ResearchersPages/Pages/avihuk.aspx>

Supplementary Material (3 figures) for this paper is available at: <http://dx.doi.org/10.1387/ijdb.160235ak>

Accepted: 8 July, 2016

inhibition of Dscam by expression of siRNA or a dominant negative form of Dscam is sufficient to block the turning (Liu *et al.*, 2009). 5) Expression of *Dscam* in *Xenopus* neurons mediates turning toward a Netrin-1 gradient in the absence of DCC signaling (Ly *et al.*, 2008). 6) In flies, *Netrin* mutants have a similar phenotype to *Dscam* mutants. Additionally, overexpression of *Dscam* in axons that do not normally cross the midline is able to induce ectopic midline crossing (Andrews *et al.*, 2008).

All these data are consistent with Dscam as an attractive receptor for Netrin-1. However, genetic analysis of *Dscam* mutants in mice has provided only partial support for this idea. In one *Dscam* allele, *Dscam*^{2J}, increased number of spinal commissural interneurons was apparent, and mutant mice displayed motor hypertonia and lack of locomotor coordination (Lemieux *et al.*, 2016, Thiry *et al.*, 2016). In another allele, commissural axons reach and cross the floor plate and *in vitro* they show normal outgrowth in response to Netrin-1 (Palmesino *et al.*, 2012). One difference is that the *Dscam*^{2J} allele may not be a null: it contains a four base pair duplication in exon 19, leading to a frameshift and truncation of the open reading frame. Hence, it is not clear whether the *Dscam*^{2J} is

a hypomorph or a neomorph.

Another possible explanation for the discrepancies is that specific subpopulations of spinal interneurons might differ in their dependence on Dscam, with alterations in one group masked by dispensability of Dscam for other groups. To explore this possibility, we selectively marked and manipulated three separate populations of dorsal spinal interneurons in chick: dl1, dl2 and dl3. The recent use of neuron-specific enhancer elements, which enables tracking of defined interneuron populations, has revealed that the dorsal interneurons dl1-3 have a different laterality preference (Avraham *et al.*, 2010a, Avraham *et al.*, 2009, Gowan *et al.*, 2001, Helms and Johnson, 1998, Reeber *et al.*, 2008). dl1 neurons project axons both ipsilaterally and contralaterally (Avraham *et al.*, 2009, Wilson *et al.*, 2008), dl2 have mostly commissural axons, while dl3 project their axons ipsilaterally (Avraham *et al.*, 2010a, Avraham *et al.*, 2009). In each case, we performed both loss- and gain-of-function tests, by either knock-down or elevation of Dscam levels in an interneuron-specific manner. We found that dl1-, dl2- and dl3-specific manipulations of *Dscam* expression did not change the trajectory choice of each of the dorsal interneuron populations.

However, Dscam was required for proper axon fasciculation.

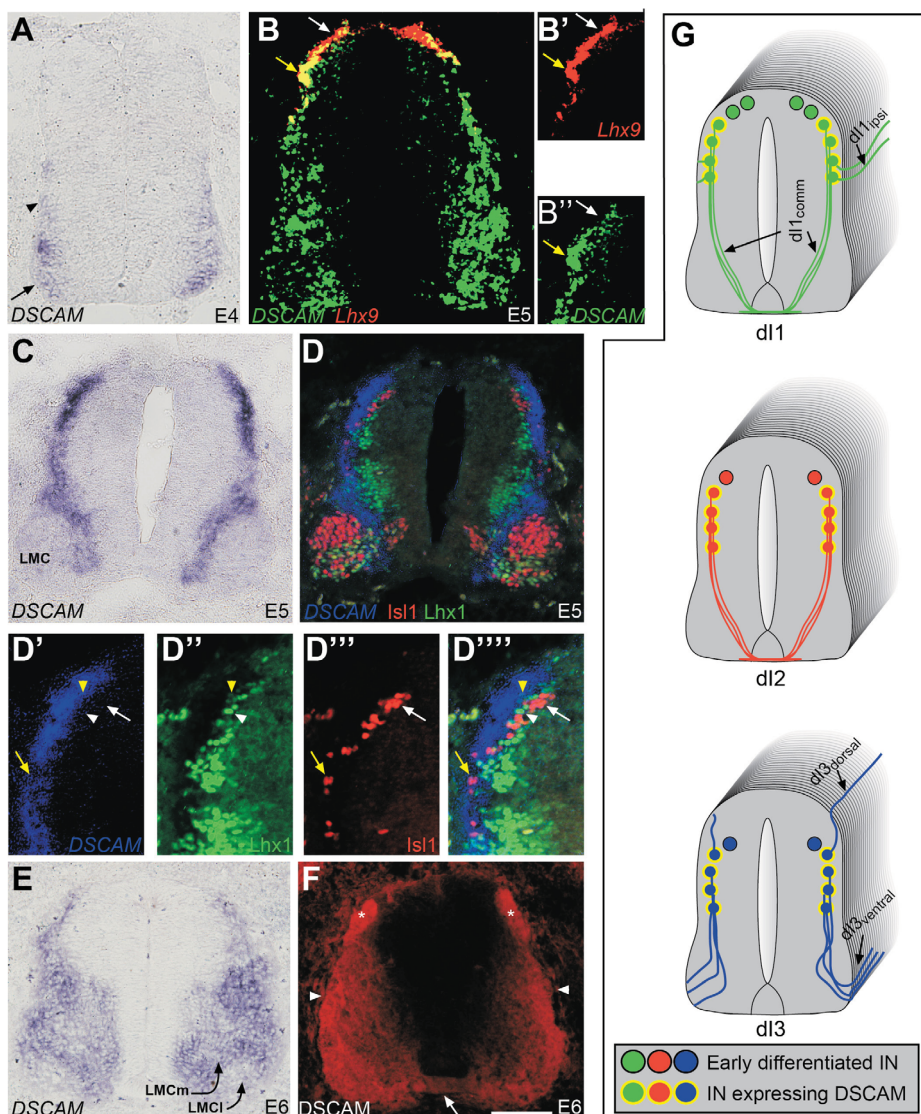
Results

Expression pattern of Dscam in the embryonic chick spinal cord

To explore whether Dscam contributes to axon growth and guidance in the chick

Fig. 1. Expression pattern of Down Syndrome cell adhesion molecule (Dscam).

In situ hybridization (A-E) and immunohistochemistry (F) were performed on cross sections of chick embryos. (A) At E4 Dscam is expressed in motor neurons (arrow) and in ventral interneurons (arrowhead). **(B)** Double in situ hybridization with Dscam (green) and Lhx9 (red). Dscam is not expressed in the early-differentiated dl1 neurons (white arrow), but is expressed in the differentiated dl1 neurons (yellow arrow). **(C)** In situ hybridization in the lumbar level of an E5 embryo. **(D)** The section in (C) was stained with antibodies against Lhx1/5 and Isl1. The bright-field image of (C) was photo-converted to a dark-field image. The early-differentiated dl2 neurons (white arrowhead) are Lhx1/5+/Dscam-, while the differentiated dl2 neurons (yellow arrowhead) are Lhx1/5+/Dscam+ (**D'**, **D''**). The early-differentiated dl3 neurons (white arrow) are Isl1+/Dscam-, while the differentiated dl3 neurons (yellow arrow) are Isl1+/Dscam+ (**D'''**, **D''''**). **(E)** At E6, Dscam is expressed at low levels in LMCi neurons and high levels in LMCm neurons. **(F)** Dscam protein is detected on axons that cross the floor plate (arrow), project ipsilaterally (arrowheads) and at the dorsal root entry zone (asterisks). **(G)** Scheme summarizing the projection pattern of dl1-3 neurons and the expression of Dscam in those neurons. Scale bar in (F) equivalent to 100 μ m for (D), 60 μ m for (D'-D'''), 200 μ m for (A), 125 μ m for (B) and 75 μ m for (E, F).



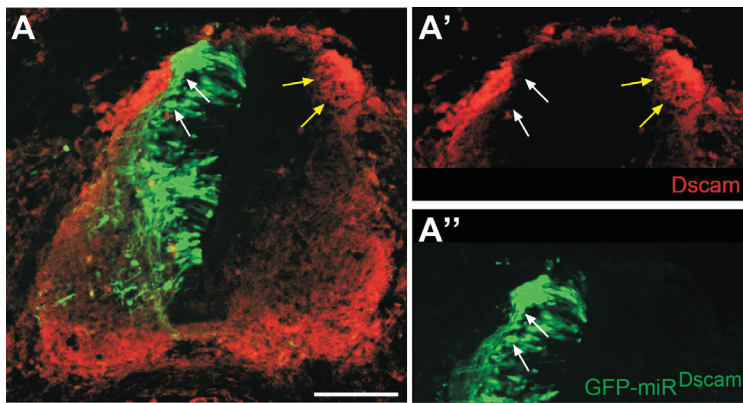


Fig. 2. The effect of miR^{Dscam} on Down Syndrome cell adhesion molecule (*Dscam*) expression. *GFP-miR^{Dscam}* cassette was expressed in the chick hemitube. A cross section stained with anti-*Dscam* is shown. At the dorsal spinal cord, neurons expressing miR^{Dscam} do not express *Dscam* (white arrows), while neurons at the dorsal part of the un-electroporated side express *Dscam* (yellow arrows). Scale bar in (A), 100 μ m.

spinal cord, we first characterized its spatial and temporal expression. *In situ* mRNA hybridization, combined with antibody staining for cell fate markers, was performed on E4-E6 chick embryo cross sections. At thoracic level of E4, *Dscam* mRNA is expressed in motor neurons and in ventral interneurons (Fig. 1A). Expression in motor neurons is observed in the thoracic-level motor neurons at E5 (Fig. 1B) and E6 (data not shown). *Dscam* is not expressed at E5 in the lateral motor column (LMC) neurons (Fig. 1 C,D). At E6, LMCI neurons express low levels, while LMCI neurons express high levels of *Dscam* (Fig. 1E). Expression in the dorsal interneurons is apparent at E5 (Fig. 1 C,D). Notably, at E4 the dorsal commissural neurons, whose axons reach the floor plate at this developmental stage, do not express detectable levels of *Dscam* (Fig. 1A).

We used cell type specific markers to verify the profile of *Dscam* expression in dl1-3 neurons. *In situ* double fluorescence hybridization to *Lhx9* and *Dscam* reveals that the most dorsal dl1 neurons, the early-differentiated dl1 neurons, do not express *Dscam*, while the lateral and more ventral differentiated dl1 neurons express *Dscam* (Fig. 1B). The expression of *Dscam* in dl2 neurons was studied using *Lhx1/5* antibody. The early-differentiated, dorsally/medially located dl2 neurons, do not express *Dscam*, while the more

lateral and ventral dl2 neurons express *Dscam* (Fig. 1D). *Isl1* was used as a dl3 neuronal marker. Consistently, expression of *Dscam* is restricted to the ventro/laterally migrating differentiated dl3 neurons (Fig. 1D). Hence, *Dscam* is expressed in the late differentiated dl1-3 neurons.

The dorsal interneurons vary in their axonal projection pattern. Along the dorsal/ventral axis, dl1c and dl2 project their axons contralaterally, while dl1i and dl3 neurons project ipsilaterally (Fig. 1G). The expression of *Dscam* protein along the axons was studied utilizing *Dscam*-specific antibody (Yamagata and Sanes, 2008). *Dscam* protein is present in the dorsal root entry zone, consistent with its expression in the DRG, in the white matter, at the lateral and ventral funiculi, where the longitudinal ipsilateral axons project, and at the floor plate, the crossing zone of the commissural axons (Fig. 1F). Thus, *Dscam* is expressed in both commissural and ipsilaterally projecting neurons and along their axons.

Strategies for loss and gain of function of *Dscam* in the chick spinal cord

We previously used a plasmid-based electroporation approach for knock-down and ectopic expression of *Dscam* in the chick retina (Yamagata and Sanes, 2008). Here, we used micro-RNA targeting *Dscam* (miR^{Dscam}) and a *Dscam* cDNA, both under the regulation of the CAGG enhancer/promoter or interneuron-specific enhancers, for loss and gain of function (Table 1). To assess our ability to down-regulate *Dscam* expression in the spinal cord, spinal cords of chick embryos were electroporated at Hamburger-Hamilton Stage 18. At E6, embryos were removed, fixed and analyzed for *Dscam* protein expression. Electroporation of spinal neurons with miR^{Dscam} decreased the expression of the *Dscam* in the soma and axons (Fig. 2A).

Dscam is not required or sufficient for the selection of axonal trajectories by dl1 neurons

To manipulate specific interneurons, we subcloned the miR^{Dscam} cassette in a Cre-dependent plasmid or a Cre/Gal4 double conditional plasmid (Avraham *et al.*, 2009), using the approach of Wilson and Stoeckli (2011). For dl1-specific perturbations, the Cre-conditional miR^{Dscam} plasmid was electroporated along with a *Edl1::Cre* plasmid (Avraham *et al.*, 2009) (Table 1, Fig. 3E). The size of the spinal cords of miR^{Dscam} and control GFP-electroporated embryos was comparable, indicating no general effect on develop-

TABLE 1

PLASMIDS USED FOR KNOCK-DOWN AND ECTOPIC EXPRESSION OF *DSCAM*

Neuron	Enhancers	Target plasmids for loss of function	Target plasmids for gain of function	Fig.
dl1	Edl1::Cre	CAG::GFP-miR ^{Dscam}		2B,D
		CAG::STOP ^{LoxP} -taumyc		
		CAG::STOP ^{LoxP} -GFP-miR ^{Dscam}	CAG::Dscam-IRES-GFP	2C
	Edl1::Gal4		UAS::mCherry-2A-Dscam	3D,G
dl1	Edl1::Cre Edl1::Gal4	UAS::taumyc ^{LoxP} -GFP-miR ^{Dscam}		6B
dl2	Edl1/2::Cre Edl2/V1::Gal4	UAS::STOP ^{LoxP} -GFP-miR ^{Dscam}		4B,E
			UAS::STOP ^{LoxP} -mCherry-2A-Dscam	4C,E
dl3	215::Gal4 242::Cre	UAS::STOP ^{LoxP} -GFP-miR ^{Dscam}		5B,E
			UAS::STOP ^{LoxP} -mCherry-2A-Dscam	5C,E

ment (Fig. 3 A-D). The ratio of ipsilaterally projecting axons from the total longitudinal axons did not differ between miR^{Dscam} and control GFP-electroporated embryos (Fig. 3A,B,F, Fig. S1A, Table 2). Likewise, the ectopic expression of *Dscam* in dl1 neurons did not alter the ipsi/contralateral ratio of dl1 axons. The ratio of ipsi/

total-projecting dl1 axons was similar between the *Dscam* over-expressing dl1 neurons and control dl1 neurons (Fig. 3 C,D,G, Fig. S1B, Table 2). Thus, neither down- nor up-regulation of *Dscam* in dl1 neurons significantly affects the ipsi- versus contralateral choice of dl1 neurons.

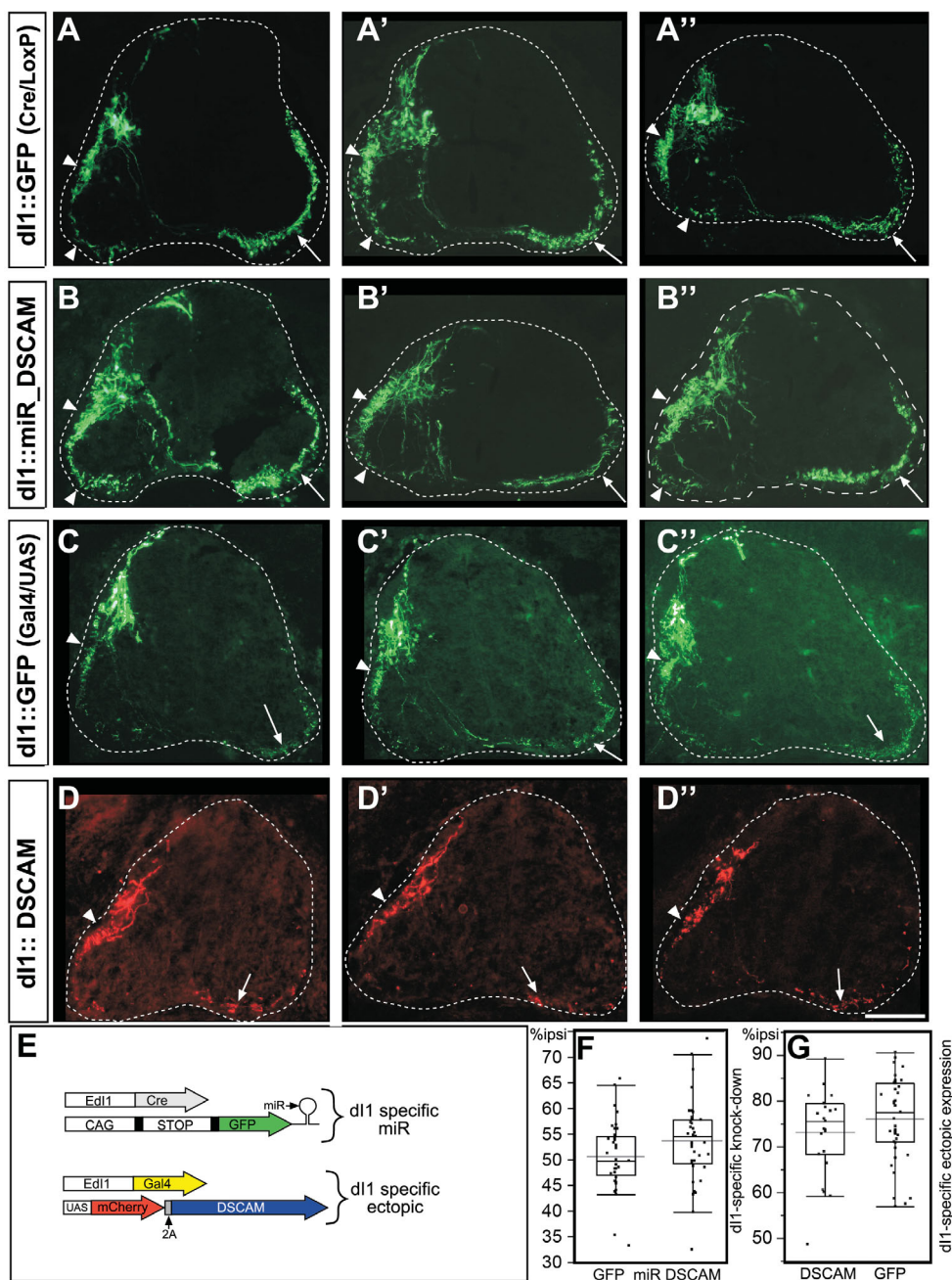


Fig. 3. Loss and gain of function of *Dscam* in dl1 neurons. Using the plasmids illustrated in (E), *Dscam* levels were down- (B) and up- (D) regulated. GFP expressed by the same drivers (Cre for A,B and Gal4 for C,D) was used as a control. Three representative images from each group are shown. White arrows point to the contralaterally projecting axons. Arrowheads point to the ipsilaterally projecting axons. (E) Schemes showing the molecular strategies for manipulating *Dscam* levels in dl1 neurons. (F) Quantification of the ipsilaterally projecting dl1 axons following knockdown of *Dscam* in dl1 neurons. A t-test was performed to compare the adjusted %ipsi of the miR^{Dscam} to the Control group. The two groups do not appear to be significantly different for $\alpha=0.05$ (p -value=0.074). (G) Quantification of the ipsilaterally projecting dl1 axons following ectopic expression of *Dscam* in dl1 neurons. A t-test was performed to compare the adjusted %ipsi of the *Dscam* to the GFP group. The groups do not appear to be statistically different (p -value=0.226). Box plot charts (G,H): The boxes, enclose 50% of the results; the horizontal lines above and under the box enclose 90% of the results; the black and gray horizontal lines within the box are the average and the median, respectively. Scale bar in (D), 125 μ m.

TABLE 2

SUMMARY OF THE STATISTICAL ANALYSIS

Fig.	Statistical test	Dependent Variable	Significance	Summary statistics*			
				Group	N	Mean	Std Dev
3F	Dunnett's test	%ipsi	No (P=0.074)	GFP	38	50.66	6.67
				miR ^{Dscam}	39	53.70	7.94
3G	Dunnett's test	%ipsi	No (P=0.226)	DSCAM	23	73.18	9.28
				GFP	41	76.07	8.99
4	Dunnett's test	%comm	Yes, for both (multiple comparisons, controls for the overall alpha level of 0.05. see fig 4E)	GFP	33	92.10	3.73
				ectopic <i>Dscam</i>	25	88.43	5.44
				miR ^{Dscam}	53	89.30	5.85
5	Dunnett's test	%ipsi	miR ^{DSCAM} is different and ectopic DSCAM is not significantly different from the control (multiple comparisons, controls for the overall alpha level of 0.05. see fig 5E)	GFP	21	97.44	0.99
				ectopic <i>Dscam</i>	16	97.13	1.52
				miR ^{Dscam}	35	98.19	0.84
6	paired T-Test	The width of miR ^{Dscam} and taumyc axonal bundle	Yes (P<0.0001)	miR ^{Dscam} minus taumyc	14	34.29	19.10

*For Figures 3-5, after adjustment for embryo effect

Dscam is not required or sufficient for the commissural axon projection of *dl2* neurons

To direct *dl2*-specific knockdown in *dl2* neurons, the miR^{Dscam} cassette was subcloned into a Gal4/Cre dual conditional vector. The dual conditional miR^{Dscam} plasmid was co-electroporated with the *dl2* enhancers plasmid-mix (Avraham *et al.*, 2009) (Table 1, Fig. 4D). A robust commissural projection following *Dscam* knockdown was observed in *dl2* neurons (Fig. 4A,B). The majority of *dl2* axons projected contralaterally following *dl2*-specific expression of either GFP, miR^{Dscam}, or *Dscam* (92.2+/-3.7%, 89.3+/-5.9% and 88.4+/-5.4%, respectively; Fig. 4 C,E, Fig. S2, Table 2). Statistical comparisons with a control using Dunnett's Method demonstrated a minor, though statistically significant, difference between the control and the manipulated *dl2* axons. However, we observed no qualitative alteration in the trajectory of *dl2* axons toward and across the floor plate. nor was there a significant difference in the commissural ratio between

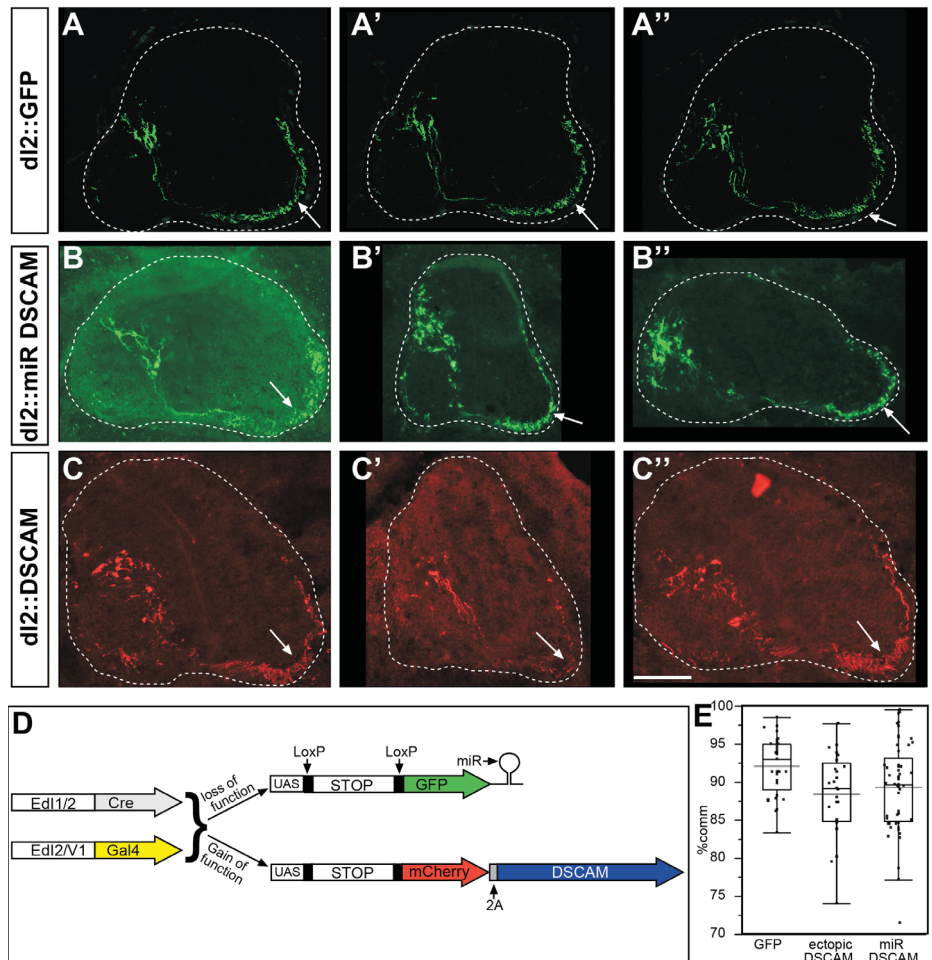
the gain and loss of function groups.

Dscam is not required or sufficient for the ipsilateral axonal projection of *dl3* neurons

The dual conditional miR^{Dscam} plasmid and the ectopic *Dscam* were co-electroporated with the *dl3* enhancer plasmid mix (Table 1, Fig. 5D). A robust ipsilateral preference was observed for *dl3* axons in both control and manipulated embryos (Fig. 5A-C). The percentage of ipsilaterally projecting axons were: 97.44+/-0.99% in the control embryos, 98.19+/-0.84% in the miR^{Dscam} expressing

Fig. 4. Loss and gain of function of *Dscam* in *dl2* neurons.

Using the plasmids illustrated in (D), *Dscam* levels were down- (B) and up- (C) regulated in *dl2* neurons. GFP expressed by the same drivers was used as a control (A). Three representative images from each group are shown. White arrows point to the contralaterally projecting axons. (D) Schemes showing the molecular strategies for manipulating *Dscam* levels in *dl2* neurons. (E) Quantification of the contralaterally projecting *dl2* axons following knockdown and ectopic expression of *Dscam*. The difference between the ectopic and the miR^{DSCAM} groups and the control group was assessed using the Dunnett's test (multiple comparisons). The test compares each level to the control level and controls for the overall alpha level (with an alpha of 0.05). The ectopic and the miR^{DSCAM} groups are significantly different from the control group (*p*-value=0.017 and 0.032 respectively). Box plot chart (E): The boxes, enclose 50% of the results; the horizontal lines above and under the box enclose 90% of the results; the black and gray horizontal lines within the box are the average and the median, respectively. Scale bar in (C), 125 μ M.



embryos, and $97.13 \pm 1.52\%$ in the ectopic *Dscam* treated embryos (Fig. 5E, Fig. S3, Table 2). Levels of crossing were significantly lower in the miR*Dscam* group than in controls, but since $>97\%$ of axons remained ipsilaterally in controls, the difference was of necessity small. Perhaps more noteworthy is the failure of *Dscam* overexpression to promote crossing of a statistically significant number of additional axons. Thus, our data provide little support for a role of *Dscam* in the crossing of dl3 axons.

Dscam is required for axonal fasciculation

The axons of dl1-3 neurons form cell type specific fascicles (Avraham et al., 2010a, Avraham et al., 2009). *Dscam*, which mediates homophilic interactions (Yamagata and Sanes, 2008), could contribute to fasciculation. To test *Dscam*'s possible role in this process, we designed a double labeling paradigm that enables simultaneous detection of wild type and knock-down mutated neurons (WT/KD plasmid). A cassette of *taumyc* reporter gene flanked

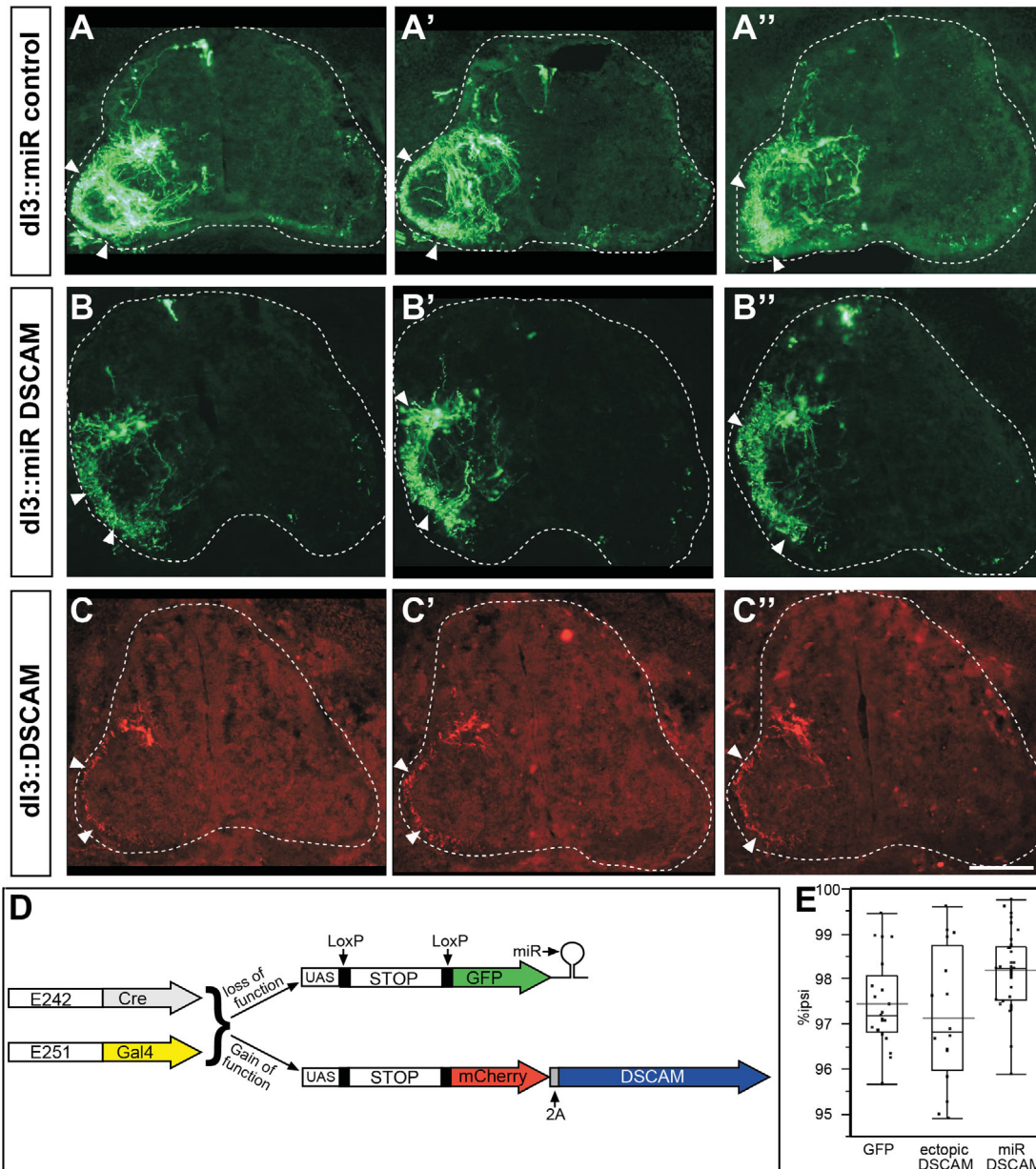


Fig. 5. Loss and gain of function of *Dscam* in dl3 neurons. Using the plasmids illustrated in (D), *Dscam* levels were down- (B) and up- (C) regulated in dl3 neurons. GFP expressed by the same drivers was used as a control (A). Three representative images from each group are shown. White arrowheads point to the ipsilaterally projecting axons. (D) Schemes showing the molecular strategies for manipulating *Dscam* levels in dl3 neurons. (E) Quantification of the ipsilaterally projecting dl3 axons following knockdown and ectopic expression of *Dscam*. The difference between the ectopic and the miR^{DSCAM} groups and the control group was assessed using the Dunnett's test (multiple comparisons). The test compares each level to the control level and controls for the overall alpha level (with an alpha of 0.05). The miR^{DSCAM} group is significantly different than the control (p -value=0.026) whereas the ectopic group is not statistically significantly different (p -value=0.581). Box plot chart (E): The boxes, enclose 50% of the results; the horizontal lines above and under the box enclose 90% of the results; the black and gray horizontal lines within the box are the average and the median, respectively. Scale bar in (C), 125 μ M.

by LoxP sites and proceeded by EGFP (EGFP-miR^{Dscam}) was cloned downstream to UAS promoter (Fig. 6C). The WT/KD plasmid was co-electroporated with Edl1-driven Cre and Gal4 plasmids to drive expression in dl1 neurons. Neurons that incorporate all the three plasmids will express EGFP-miR^{Dscam} and consequently will down regulate *Dscam* expression, while neurons that incorporate only the Edl1::Gal4 and WT/KD plasmids will express *taumyc*. Other combination of plasmids will not lead to expression of either the reporter or the miR^{Dscam} cassette. We excluded axons that expressed both EGFP and *taumyc*; they likely initiated expression of *taumyc* early, and only subsequently activated the miR^{Dscam} via

late expression of Cre.

The main result was that the *Dscam*-deficient (EGFP-positive) axons were spread over a broader area than the control (*taumyc*-positive) axons (Fig. 6A,B). To quantify the difference, we measured the width (in pixels) of the dl1 axon bundle at the circumferential axis (Fig. 6D). The average width of miR^{Dscam} dl1 bundle was 2.05 ± 0.86 times greater than the width of the control bundle.

Due to the fact that the wild type and mutated axons differ from each other regarding their fasciculation, the statistical analysis was performed in the following manner: the width of miR^{Dscam} and the control (*taumyc* expressing axons) were scored per section.

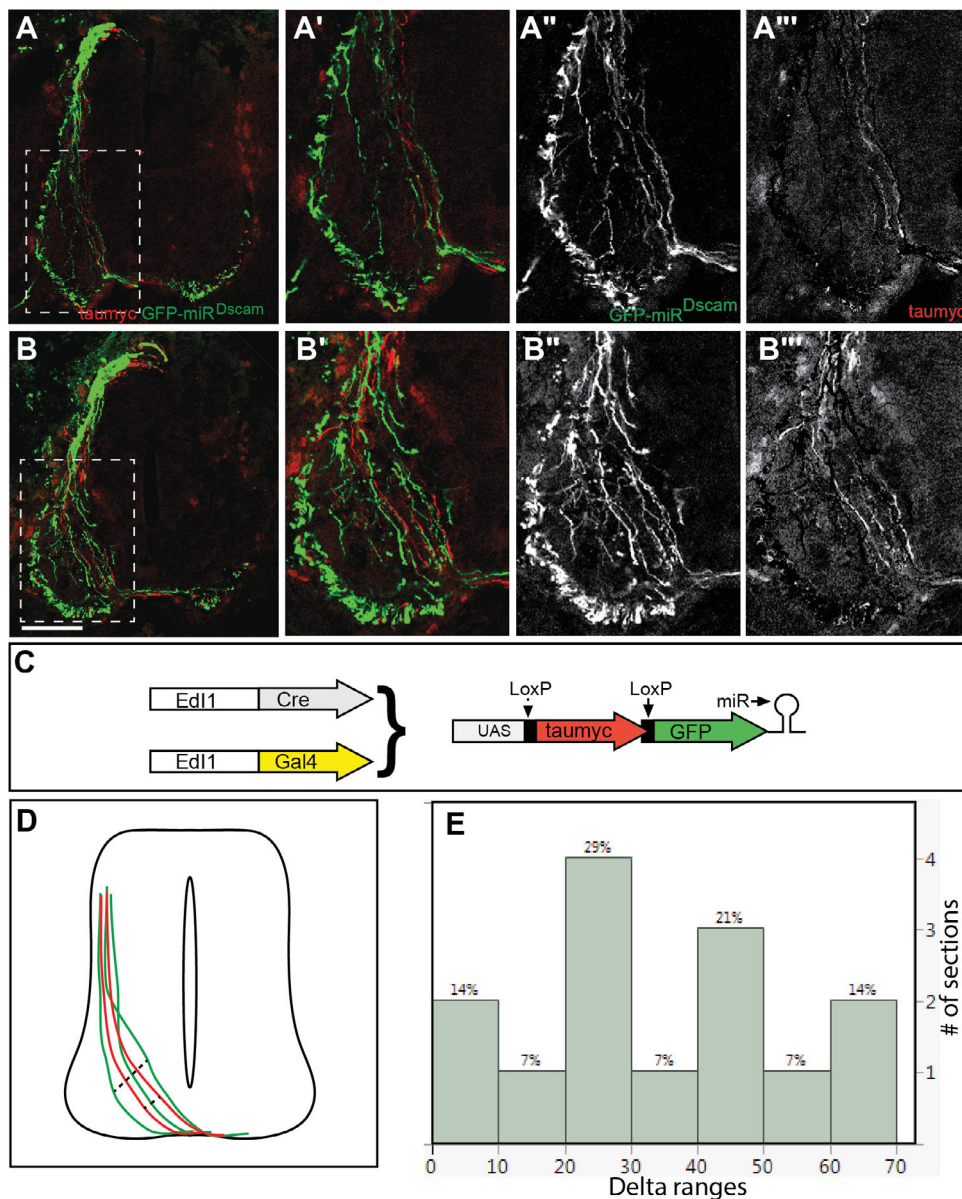


Fig. 6. Knockdown of *Dscam* results in widening of dl1 axonal fascicle. Using the plasmids illustrated in (C), a chimeric axonal genotype of dl1 neurons was obtained: Wild type dl1 neurons expressing miR^{DSCAM} and mutated dl1 neurons expressing GFP-miR^{DSCAM}. The wide fanning of GFP-miR^{DSCAM} axons (A,A',A'',B,B',B'',B''') versus the tight bundle of the wild type, *taumyc*-expressing axons (A'',B'''), is evident. The width of the bundles was measured as illustrated (D). The chart (E) shows the histogram of the differences. The X axis shows delta ranges - the width of the miR^{Dscam} fasciculus minus the width of *taumyc* fasciculus (width measured as pixels). The Y axis shows the counts (number of samples). Above each bar the percent of sections is specified. Scale bar in (A), 100 μ m for (A) and 60 μ m for (A'-A''').

Deltas (the width of miR^{Dscam} fascicle minus taumyc fascicle) were evaluated per image. Thus, if the two groups widths were similar, these deltas would tend to be distributed around zero, while larger deltas would indicate larger miR^{Dscam} widths compared to the control. Deltas evaluated from the 14 sections, range between 7 and 32 with an average of 34.3 +/- 19.1. A T-Test was used for testing the null hypothesis that the deltas are zero. The test showed a statistically significant result, rejecting the null hypothesis ($P < 0.0001$). (Fig. 6E, table 2). Therefore, we concluded that the width of miR^{Dscam} dl1 axons was significantly larger than that of control axons. Thus, *Dscam* is required for the fasciculation of dl1 axons as they project toward the floor plate.

Discussion

Genetic evidence in the fly supports the role of *Dscam* in the guidance of embryonic commissural axons by Netrin-1 dependent and independent modes (Andrews *et al.*, 2008). In vertebrates, down-regulation of *Dscam*, via siRNA treatment, was shown to inhibit the axonal growth of dorsal interneurons toward the floor plate in mouse and chick (Liu *et al.*, 2009, Ly *et al.*, 2008). Conversely, the *in vivo* requirement of *Dscam* for commissural guidance in vertebrates was contested in a recent paper that used a null allele, which reported a normal projection pattern of spinal commissural axons in the (Palmesino *et al.*, 2012).

We have reexamined the role of *Dscam* in the guidance of chick spinal interneurons using cell-type specific knock-down and ectopic expression strategies. The loss and gain of function tools used in this study were previously utilized to demonstrate the requirement of *Dscam* for directing the lamina-specific synaptic connection of *Dscam*-expressing retinal ganglion cells (Yamagata and Sanes, 2008). A Knock-down of *Dscam* in the commissural interneurons, dl1c and dl2, did not prevent their extension toward and across the floor plate. Complementary, ectopic expression of *Dscam* in the ipsilaterally projecting populations, dl1i and dl3, did not alter their ipsilateral projection. Though, we argue that as in the mouse, also in the chick spinal cord *Dscam* is not involved in attraction to the floor plate. In addition, we have demonstrated that the ipsilateral projection of dl1c and dl3 neurons is not altered following *Dscam* knockdown, and the commissural projection of dl1c and dl2 is not affected succeeding ectopic expression of *Dscam*. Providing evidence for the dispensability of *Dscam* for midline repulsion of ipsilateral projecting neurons, which was not addressed in the mouse genetic model (Palmesino *et al.*, 2012). Our results do not provide substantial support for the idea that *Dscam* serves as a neuronal receptor for cues that promote midline crossing of spinal interneurons. In this respect, our conclusions are consistent with those of Palmesino *et al.*, (2008). On the other hand, we did observe small but statistically significant decreases or increase in crossing when *Dscam* levels were decreased in dl2 and dl3 neurons, respectively. We were unable to obtain a quantitative measure of the extent of *Dscam* attenuation in these neurons. Therefore, we cannot formally exclude the possibility that more complete inhibition might have led to a more dramatic effect. New gene editing tools will provide a means of testing this possibility in the future.

The binding of netrin-1 to *Dscam* was shown using diverse biochemical and cell biology means (Andrews *et al.*, 2008, Liu *et al.*, 2009, Ly *et al.*, 2008). Genetic evidence in flies supports the

role of *Dscam* in mediating attraction toward the midline-derived Netrin molecules (Andrews *et al.*, 2008). An additional interpretation for Netrin/*Dscam* interaction is suggested: *Dscam*1 functions to counter *Drosophila* sensory neuron dendritic targeting signals provided by secreted Netrin-B and Frazzled. Loss of *Dscam*1 function resulted in Frazzled-dependent aberrant dendrite accumulation at a Netrin-B-expressing target (Matthews and Grueber, 2011). The counter-netrin activity of *Dscam* may reside from competition on Netrin binding between *Dscam* and Fra/DCC. Since the affinity to Netrin of both receptors is similar, higher levels of *Dscam* will sequester Netrin from binding the Fra/DCC. Alternatively, *Dscam*-mediated self-avoidance that is triggered by homophilic binding of *Dscam*, may initiate a signaling cascade that inhibits the Netrin/DCC signaling pathway. The relative balance between the levels of *Dscam* and DCC can shift the equilibrium between attraction and repulsion in this model as well.

Netrin-1/*Dscam* interaction in vertebrates may modulate Netrin-1 activity at other, post floor plate, choice points along the pathway. The possible role of *Dscam* in the guidance of the axons along the late longitudinal segments rather than the early circumferential segment of their projection, relies on the temporal profile of *Dscam* expression. At E4, when commissural axons cross the floor plate, *Dscam* is not expressed in the dorsal interneurons (Fig. 1A). At E5, *Dscam* expression is absent in the early-differentiated commissural interneurons that project toward the floor plate, while its expression is up-regulated in the presumed post-crossing late-differentiated neurons (Fig. 1 B-D). *Dscam* may participate in silencing netrin-1 responsiveness in post-floor plate-crossing commissural axons.

Homophilic interaction between *Dscam* expressing neurons was demonstrated in the chick and mouse retina. Our results highlight the homophilic activity also in the wiring of spinal interneurons. The novel wild type/knockdown chimeric system (Fig. 6) that we have developed assisted in revealing the requirement of *Dscam* for axonal fasciculation of dl1 axons. Scoring the phenotype of wild type and mutated neurons, within the same specimen, is advantageous over using control and manipulated chick embryos, since the efficiency of gene delivery may vary significantly between embryos. Applying this method is currently limited to neurons that can be targeted by a single enhancer. Hence, the possible role of *Dscam* in the fasciculation of dl2 and dl3, as well as in other spinal interneurons was not addressed in the current study. Therefore, we cannot exclude a dl1-specific role of *Dscam* in axonal fasciculation. Notably, no fasciculation defects, in TAG expressing commissural axons, were reported in the *Dscam* null mouse (Palmesino *et al.*, 2012). The discrepancy may arise from the fact that dl1 are only a fraction of commissural axons, and their projection is obscure by other commissural axons.

The responsiveness of growth cones to guidance cues is context-dependent. Repulsion from- versus attraction to- a defined guidance molecule can be gated by different receptor complexes or different intracellular signaling pathways (Dickson and Zou, 2010, Evans and Bashaw, 2010). Similarly, adhesive and repellent interactions between axons, that leads to either fasciculation or defasciculation, respectively, are also context-dependent. Role for *Dscam* in adhesive interaction in the retina (Yamagata and Sanes, 2008), as well as a repulsive molecule that prevents fasciculation of RGC's dendrites (Fuerst *et al.*, 2009), was demonstrated. Likewise, in *Drosophila*, *Dscam* is implicated in dendrites avoidance

(Matthews *et al.*, 2007) as well as attraction (Tadros *et al.*, 2016). It is not yet clear what controls the opposing activities of Dscam.

Dscam is expressed in numerous interneurons in the spinal cord, which raises the question whether Dscam can serve as a cell type specific fasciculation factor. Expression of other Ig-super family molecules that share the homophilic interaction activity: Sidekicks and Contactins, is more restricted in the spinal cord. Hence, a combinatorial expression of DSCAM/Sdk and Contactins may serve as homophilic code for self fasciculation of axonal bundle in the spinal cord, as it was shown in the retina (Yamagata and Sanes, 2012).

Materials and Methods

DNA

The GFP-miR-Dscam-b cassette (Yamagata and Sanes, 2008), was amplified by PCR using forward [ATGCTAGCAAAACCATGGTGAGCAAGGG] and reverse [ATGCGGCCGCTAGATATCTCGAGTGCGGCC] primers. PCR product was digested with NheI and NotI and subcloned into a Cre or Gal4/Cre dependent plasmids (Avraham *et al.*, 2009, Hadas *et al.*, 2014). The mCherry-2A-Dscam cassette (Yamagata and Sanes, 2008) was excised by EcoRI+NotI digest and subcloned downstream to the UAS promoter. Plasmids containing dl1, dl2 and dl3 enhancers driving Cre and Gal4 were described previously (Avraham *et al.*, 2010a, Avraham *et al.*, 2009, Hadas *et al.*, 2014).

In ovo electroporations

Fertilized White Leghorn chicken eggs were incubated at 38.5-39°C. A DNA solution of 5 mg/ml was injected into the lumen of the neural tube stage 17-18. Electroporation was performed using 3 x 50 ms pulses at 30V, applied across the embryo using a 0.5 µm Tungsten wire and a BTX electroporator (ECM 830). Embryos were incubated for 3 days prior to analysis (Avraham *et al.*, 2010b).

Immunohistochemistry

Embryos were fixed overnight at 4°C in 4% paraformaldehyde/0.1 M phosphate buffer, washed twice with PBS, incubated in 30% sucrose/PBS for 24 hours, and embedded in OCT. Cryostat sections (14 µm) were collected on Superfrost Plus slides and kept at -70°C. The following antibodies were used: rabbit polyclonal GFP antibody (Molecular Probes), Lhx2/9, Lhx1/5, Isl1 (provided by T. Jessell, Columbia University, New York, NY) Dscam (Medimabs, Montreal). Cy2, RRX and cy5 were used as fluorochromes. Images were captured under a microscope (Axioscope 2; Zeiss) with a digital camera (DP70; Olympus) or confocal microscope (FV1000; Olympus).

For *in situ* double mRNA fluorescence the Tyramide Signal Amplification (TSA) kit (Perkin Elmer) was used. For double: mRNA *in situ* + immunohistochemistry, the traditional dig-AP (Roche) protocol was used. Following the AP color reaction, slides were incubated with the appropriate antibody as described above.

Quantification

Each experiment included both manipulated and control groups, which were electroporated within two hours of each other. Comparisons were made between manipulated and control embryos within an experiment. For each group 2-5 embryos were electroporated. At E6 embryos were removed from the eggs, fixed and sectioned. In each cross section the number of axons projecting longitudinally was scored. The number of pixels in the white matter at the ipsilateral and contralateral was calculated using ImageJ tools.

Analysis methodology: In some instances, there was a large embryo to embryo variability within groups. Thus, the analyses were performed on adjusted data, after removing the embryo effect. T-test was applied on the adjusted values to compare between two groups. In the cases

of three groups, where each level is compared to a control, the multiple comparisons Dunnett's test was used. The charts show the adjusted values. In the supplementary figures, both the original values and the embryo data are presented.

Acknowledgements

The authors thank Artur Kania, Oshri Avraham and Yoav Hadas for comments on the manuscript. This work was supported by grants to AK and JS from the BSF (2013/058), AK from the Israel Science Foundation (grant No. 229/09 and 631/13) and AK from the Ida and Avraham Baruch Endowment Fund.

References

- ANDREWS, G.L., TANGLAO, S., FARMER, W.T., MORIN, S., BROTMAN, S., BERBEROGLU, M.A., PRICE, H., FERNANDEZ, G.C., MASTICK, G.S., CHARRON, F. *et al.*, (2008). Dscam guides embryonic axons by Netrin-dependent and -independent functions. *Development* 135: 3839-3848.
- AVRAHAM, O., HADAS, Y., VALD, L., HONG, S., SONG, M.R. and KLAR, A. (2010a). Motor and dorsal root ganglia axons serve as choice-points for the ipsi-lateral turning of dl3 axons. *J. Neurosci.* 30: 15546-15557.
- AVRAHAM, O., HADAS, Y., VALD, L., ZISMAN, S., SCHEJTER, A., VISEL, A. and KLAR, A. (2009). Transcriptional control of axonal guidance and sorting in dorsal interneurons by the Lim-HD proteins Lhx9 and Lhx1. *Neural Dev* 4: 21.
- AVRAHAM, O., S. ZISMAN, Y. HADAS, L. VALD and A. KLAR (2010). Deciphering axonal pathways of genetically defined groups of neurons in the chick neural tube utilizing *in ovo* electroporation. *J Vis Exp* 39: 1792. (doi: 10.3791/1792)
- CHARRON, F., STEIN, E., JEONG, J., MCMAHON, A.P. and TESSIER-LAVIGNE, M. (2003). The morphogen sonic hedgehog is an axonal chemoattractant that collaborates with netrin-1 in midline axon guidance. *Cell* 113: 11-23.
- DICKSON, B.J. and ZOU, Y. (2010). Navigating intermediate targets: the nervous system midline. *Cold Spring Harb Perspect Biol* 2: a002055.
- EVANS, T.A. and BASHAW, G.J. (2010). Axon guidance at the midline: of mice and flies. *Curr Opin Neurobiol* 20: 79-85.
- FAZELI, A., DICKINSON, S.L., HERMISTON, M.L., TIGHE, R.V., STEEN, R.G., SMALL, C.G., STOECKLI, E.T., KEINO-MASU, K., MASU, M., RAYBURN, H. *et al.*, (1997). Phenotype of mice lacking functional Deleted in colorectal cancer (Dcc) gene. *Nature* 386: 796-804.
- FUERST, P.G., BRUCE, F., TIAN, M., WEI, W., ELSTROTT, J., FELLER, M.B., ERSKINE, L., SINGER, J.H. and BURGESS, R.W. (2009). DSCAM and DSCAML1 function in self-avoidance in multiple cell types in the developing mouse retina. *Neuron* 64: 484-497.
- GOWAN, K., HELMS, A.W., HUNSAKER, T.L., COLLISSON, T., EBERT, P.J., ODOM, R. and JOHNSON, J.E. (2001). Crossinhibitory activities of Ngn1 and Math1 allow specification of distinct dorsal interneurons. *Neuron* 31: 219-232.
- HADAS, Y., ETLIN, A., FALK, H., AVRAHAM, O., KOBILER, O., PANET, A., LEVTOV, A. and KLAR, A. (2014). A 'tool box' for deciphering neuronal circuits in the developing chick spinal cord. *Nucleic Acids Res.* 42: e148.
- HELMS, A.W. and JOHNSON, J.E. (1998). Progenitors of dorsal commissural interneurons are defined by MATH1 expression. *Development* 125: 919-928.
- KENNEDY, T.E., SERAFINI, T., DE LA TORRE, J.R. and TESSIER-LAVIGNE, M. (1994). Netrins are diffusible chemotropic factors for commissural axons in the embryonic spinal cord. *Cell* 78: 425-435.
- LEMIEUX, M., O, D.L., THIRY, L., BOULANGER-PIETTE, A., FRENETTE, J. and BRETZNER, F. (2016). Motor hypertonia and lack of locomotor coordination in mutant mice lacking DSCAM. *J Neurophysiol* 115: 1355-1371.
- LIU, G., LI, W., WANG, L., KAR, A., GUAN, K.L., RAO, Y. and WU, J.Y. (2009). DSCAM functions as a netrin receptor in commissural axon pathfinding. *Proc Natl Acad Sci USA* 106: 2951-2956.
- LY, A., NIKOLAIEV, A., SURESH, G., ZHENG, Y., TESSIER-LAVIGNE, M. and STEIN, E. (2008). DSCAM is a netrin receptor that collaborates with DCC in mediating turning responses to netrin-1. *Cell* 133: 1241-1254.
- MATTHEWS, B.J. and GRUEBER, W.B. (2011). Dscam1-Mediated Self-Avoidance Counters Netrin-Dependent Targeting of Dendrites in *Drosophila*. *Curr Biol* 21: 1480-1487.

- MATTHEWS, B.J., KIM, M.E., FLANAGAN, J.J., HATTORI, D., CLEMENS, J.C., ZIPURSKY, S.L. and GRUEBER, W.B. (2007). Dendrite self-avoidance is controlled by Dscam. *Cell* 129: 593-604.
- OKADA, A., CHARRON, F., MORIN, S., SHIN, D.S., WONG, K., FABRE, P.J., TESSIER-LAVIGNE, M. and MCCONNELL, S.K. (2006). Boc is a receptor for sonic hedgehog in the guidance of commissural axons. *Nature* 444: 369-373.
- PALMESINO, E., HADDICK, P.C., TESSIER-LAVIGNE, M. and KANIA, A. (2012). Genetic analysis of DSCAM's role as a Netrin-1 receptor in vertebrates. *J Neurosci* 32: 411-416.
- REEBER, S.L., SAKAI, N., NAKADA, Y., DUMAS, J., DOBRENIS, K., JOHNSON, J.E. and KAPRIELIAN, Z. (2008). Manipulating Robo expression *in vivo* perturbs commissural axon pathfinding in the chick spinal cord. *J Neurosci* 28: 8698-8708.
- RUIZ DE ALMODOVAR, C., FABRE, P.J., KNEVELS, E., COULON, C., SEGURA, I., HADDICK, P.C., AERTS, L., DELATTIN, N., STRASSER, G., OH, W.J. *et al.*, (2011). VEGF mediates commissural axon chemoattraction through its receptor Flk1. *Neuron* 70: 966-978.
- SERAFINI, T., COLAMARINO, S.A., LEONARDO, E.D., WANG, H., BEDDINGTON, R., SKARNES, W.C. and TESSIER LAVIGNE, M. (1996). Netrin-1 is required for commissural axon guidance in the developing vertebrate nervous system. *Cell* 87: 1001-1014.
- SERAFINI, T., KENNEDY, T.E., GALKO, M., MIRZAYAN, C., JESSELL, T.M. and TESSIER-LAVIGNE, M. (1994). The netrins define a family of axon outgrowth-promoting proteins homologous to *C. elegans* UNC-6. *Cell* 78: 409-424.
- TADROS, W., XU, S., AKIN, O., YI, C.H., SHIN, G.J., MILLARD, S.S. and ZIPURSKY, S.L. (2016). Dscam Proteins Direct Dendritic Targeting through Adhesion. *Neuron* 89: 480-493.
- THIRY, L., LEMIEUX, M., O, D.L. and BRETZNER, F. (2016). Role of DSCAM in the development of the spinal locomotor and sensorimotor circuits. *J Neurophysiol* 115: 1338-1354.
- WILSON, N.H. and STOECKLI, E.T. (2011). Cell type specific, traceable gene silencing for functional gene analysis during vertebrate neural development. *Nucleic Acids Res.*
- WILSON, S.I., SHAFER, B., LEE, K.J. and DODD, J. (2008). A molecular program for contralateral trajectory: Rig-1 control by LIM homeodomain transcription factors. *Neuron* 59: 413-424.
- YAMAGATA, M. and SANES, J.R. (2008). Dscam and Sidekick proteins direct lamina-specific synaptic connections in vertebrate retina. *Nature* 451: 465-469.
- YAMAGATA, M. and SANES, J.R. (2012). Expanding the Ig superfamily code for laminar specificity in retina: expression and role of contactins. *J Neurosci* 32: 14402-14414.

Further Related Reading, published previously in the *Int. J. Dev. Biol.*

The involvement of three signal transduction pathways in botryllid ascidian astogeny, as revealed by expression patterns of representative genes

Amalia Rosner, Gilad Alfassi, Elizabeth Moiseeva, Guy Paz, Claudette Rabinowitz, Ziva Lapidot, Jacob Douek, Abraham Haim and Baruch Rinkevich
Int. J. Dev. Biol. (2014) 58: 677-692

From Agrobacterium to viral vectors: genome modification of plant cells by rare cutting restriction enzymes

Ira Marton, Arik Honig, Ayelet Omid, Noam De Costa, Elena Marhevka, Barry Cohen, Amir Zuker and Alexander Vainstein
Int. J. Dev. Biol. (2013) 57: 639-650

What Hydra can teach us about chemical ecology – how a simple, soft organism survives in a hostile aqueous environment

Tamar Rachamim and Daniel Sher
Int. J. Dev. Biol. (2012) 56: 605-611

Analysis of chemotaxis when the fraction of responsive cells is small - application to mammalian sperm guidance

Anna Gakamsky, Edna Schechtman, S. Roy Caplan and Michael Eisenbach
Int. J. Dev. Biol. (2008) 52: 481-487

Mouse models to study inner ear development and hereditary hearing loss

Lilach M. Friedman, Amiel A. Dror and Karen B. Avraham
Int. J. Dev. Biol. (2007) 51: 609-631

The importance of the posterior midline region for axis initiation at early stages of the avian embryo

Oded Khaner
Int. J. Dev. Biol. (2007) 51: 131-137

Early stages of neural crest ontogeny: formation and regulation of cell delamination

Chaya Kalcheim and Tal Burstyn-Cohen
Int. J. Dev. Biol. (2005) 49: 105-116

Allogeneic interactions in Hydractinia: is the transitory chimera beneficial?

Sharon Gild, Uri Frank and Ofer Mokady
Int. J. Dev. Biol. (2003) 47: 433-438

High proliferation rate characterizes the site of axis formation in the avian blastula-stage embryo.

N Zahavi, V Reich and O Khaner
Int. J. Dev. Biol. (1998) 42: 95-98

